13. Prove in regard to the corollary to Theorem 4.3.5 that the subgroup of the covering transformation group $\mathscr{A}$ that leaves fixed a particular prebranch point of x must be cyclic and generated by a conjugate of the element b.

4.4. CURRENT GRAPHS

The historical origins of topological graph theory lie largely in map-coloring problems concerned with the relationships between regions on a surface. From our present perspective, it should not be surprising that duality plays a central role. In fact, the main method used in the original solution of the Heawood map-coloring problem is a dual form of the voltage graph called a "current graph". The precursors of this technique can be traced back through Ringel's work to Heffter (1891).

4.4.1. Ringel's Generating Rows for Heffter's Schemes

In trying to establish that the Heawood number for the surface S_g is the chromatic number, and not just an upper bound, Heffter (1891) sought the minimal-genus surface consisting of n regions (faces), each of which is a neighbor of all the others. Heffter did consider the problem simultaneously in primal and dual forms, and he also wished to compute the genus of the complete graph K_n. To describe the surface, he started with n $(n-1)$-sided polygons, and he labeled them $1, 2, \ldots, n$. The sides of polygon i were then labeled by

$$1, 2, \ldots, i-1, i+1, \ldots, n$$

to indicate where the neighboring polygons should be attached. Figure 4.17, which is taken from Heffter's paper, illustrates this procedure for a surface with five regions. The identifications along the sides of polygon 1 have already been made. When the remaining sides are pasted together, the segments AB and DC are identified as are the segments AD and BC, thereby yielding a torus.

For the most part, Heffter did not depend on pictures and, instead, gave a "table" of n rows, in which row i lists in cyclic order the labels for the sides of polygon i. The table he gave for the preceding example of five regions was

(1) 3 2 4 5
(2) 4 3 5 1
(3) 5 4 1 2
(4) 1 5 2 3
(5) 2 1 3 4

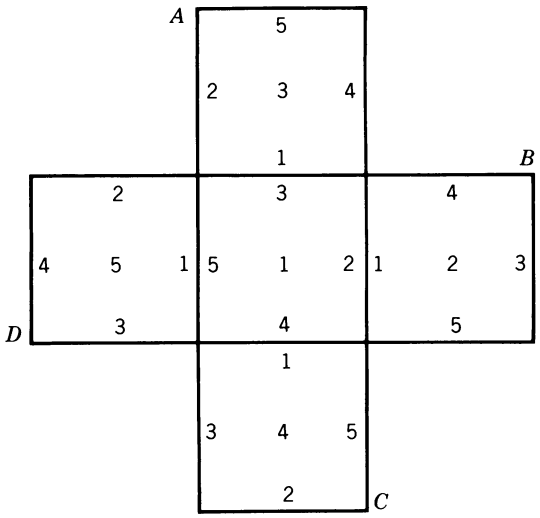

Figure 4.17. Five labeled polygons.

We now recognize such a table as a rotation system for an imbedding of the complete graph K_5, to which the mapping of Figure 4.17 is a dual. Heffter showed how the cycle of polygons meeting at a vertex can be recovered from the table; that is, he gave a face tracing algorithm for the imbedding of K_n. Having thus realized the "purely arithmetical nature of the problem", he constructed tables yielding minimal imbeddings of K_n for all $n \leq 12$. Although Ringel was well aware of Heffter's methods, their present popularity evidently rose because of the abstract of Edmonds (1960).

In addition to the use of duality and the introduction of rotation systems, it is especially noteworthy that Heffter gave tables for K_n, $n = 5, 6, 7$, in which row $i + 1$ was obtained by adding 1 modulo n to the numbers of row i. Heffter proved that such conveniently generated tables exist for general $n > 6$ only if n is of the form $12s + 7$, and he constructed them in the cases in which $4s + 3$ is prime and 2^k is not congruent to ± 1 modulo $4s + 3$ for $0 < k < 12s + 1$. (It is still not known whether there are infinitely many such s.) These tables generated from a single row using the cyclic group $\mathscr{Z}_n$ have ultimately evolved into voltage graphs. For example, the table given above for $n = 5$ is precisely the derived rotation system for the voltage graph of Example 4.1.3.

When Ringel began his work on the genus of complete graphs, he also chose to describe surfaces with tables like Heffter's, calling them "schemes". In an important generalization of Heffter's work, he designed the strategy of letting most of the rows of the scheme be generated from a small number of rows. Unlike Heffter, however, he had spectacular success with this technique. For instance, Ringel (1961) obtained the minimal imbedding of K_n for all n of the form $12s + 7$, by constructing a single generating row for the scheme that Heffter had been unable to obtain without restricting s. Despite Ringel's

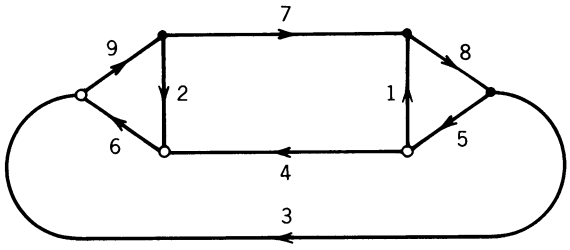

Figure 4.18. A current graph with currents in $\mathscr{Z}_{19}$.

particular brilliance in constructing such generating rows, a general method to find them was still lacking. Such a method was ultimately provided in rudimentary form by Gustin (1963).

4.4.2. Gustin's Combinatorial Current Graphs

Gustin began with a planar drawing of a graph G. At each vertex he assigned a direction, clockwise or counterclockwise. This led to what Gustin thought of as flows within the graph, which we now recognize as face boundaries. Each edge was assigned a direction and a "current", by which he meant an element of some group $\mathscr{A}$.

Example 4.4.1. *The current graph in Figure* 4.18 *leads to a single generating row for a triangular imbedding of the complete graph* K_{19} *in the surface* S_{20}. *To get that row (in our present notation), write the vertex* v_0 *at the left, which is to show which vertex has the rotation specified by the row. Then proceed as follows.*

Start at any directed edge, for instance, the one labeled with current 9 *modulo* 19. *Write that current as the subscript on the first vertex in the row. (Since the resulting graph will have no multiple edges, the entries in the rows of the scheme can be vertices, rather than directed edges.)*

At the end of that first directed edge is a filled vertex, indicating that the second edge is to be obtained by moving in a clockwise direction. That is, the directed edge with current 7 *is next, so write* v_7 *next in the generating row. Continue in this manner, going clockwise at every solid vertex* (•) *and counterclockwise at every hollow vertex* (○), *until every edge has been traversed in both directions. When proceeding in the minus direction on an edge, one writes the additive inverse modulo* 19 *of the current shown on the plus direction. The resulting generating row is*

$$v_0.\quad v_9\, v_7\, v_8\, v_3\, v_{13}\, v_{15}\, v_{14}\, v_{11}\, v_{18}\, v_4\, v_{17}\, v_{10}\, v_{16}\, v_5\, v_1\, v_{12}\, v_2\, v_6$$

The next row is

$$v_1.\quad v_{10}\, v_8\, v_9\, v_4\, v_{14}\, v_{16}\, v_{15}\, v_{12}\, v_0\, v_5\, v_{18}\, v_{11}\, v_{17}\, v_6\, v_2\, v_{13}\, v_3\, v_7$$

In general, the subscript on the jth *entry in row* v_i *is obtained by adding* i *modulo* 19 *to the subscript on the* jth *entry of row* v_0.

Gustin imposed a number of rules on the graph, on the assignment of rotations, and on the assignment of currents, whose total effect is to guarantee that the resulting scheme described an imbedding of a Cayley graph for the current group. The Kirchhoff current law (KCL) is that the sum (or product, for nonabelian currents) of the currents leaving each vertex is the group identity. Gustin's requirement that the graph be regular and that every vertex satisfy KCL has the effect of ensuring that every face in the resulting imbedding has the same number of sides as the valence of every vertex in the current graph.

Gustin's current graphs were regarded as computational tools ("nomograms" in Youngs's terminology) to aid in the construction of generating rows for schemes. Progressively more constructive power was obtained over the next few years as Gustin's original rules were relaxed. Very importantly, Youngs (1967) explained how to use current graphs with excess currents at some vertices. Whereas Gustin (1963) discussed only the cases of one, two, or three generating rows, Jacques (1969) gave a general exposition, still restricted to Cayley graphs, but covering the possibility of arbitrarily many generating rows. Finally, Gross and Alpert (1973, 1974) showed how a topological viewpoint makes it possible to eliminate all of Gustin's restrictions, and they unified all previously defined kinds of current graphs into the one now described.

4.4.3. Orientable Topological Current Graphs

Let $G \to S$ be an imbedding in an oriented surface. An "(ordinary) current assignment" is a function β from the set of directed edges of G into a group $\mathscr{B}$ such that $\beta(e^-) = \beta(e^+)^{-1}$ for every edge e. The values of β are called "currents" and $\mathscr{B}$ is called the "current group". The pair $\langle G \to S, \beta \rangle$ is called a current graph. If the clockwise and counterclockwise directions used by Gustin to order the entries in a generating row are reinterpreted as vertex rotations, the result is a legitimate imbedding. Hence, Gustin's combinatorial current graphs are properly considered a special case of a topological covering space construction.

The point of assigning currents to an imbedding is to obtain a "derived graph G_β" and "derived imbedding $G_\beta \to S_\beta$". The vertex set of G_β is the cartesian product $F_G \times \mathscr{B}$, and the edge set is the product $E_G \times \mathscr{B}$. Thus, vertices of the derived graph correspond to faces of the current graph, as in Gustin's construction. Endpoints and plus directions of derived edges are given as follows. The plus direction of the derived edge (e, b) has initial vertex (f, b) and terminal vertex (g, bc), where the rotation at the initial vertex of the directed edge e^+ carries face f to face g and $\beta(e^+) = c$. Thus, the directed edge $(e, b)^-$ goes from the vertex (g, bc) to the vertex (f, b). It will be notationally convenient to refer sometimes to the directed edge $(e, bc^{-1})^-$, which goes from vertex (g, b) to vertex (f, bc^{-1}), as (e^-, b); also, we let (e^+, b) stand for $(e, b)^+$. The rotation system for the derived imbedding is

obtained by lifting boundary walks of the imbedding $G \to S$, as follows. If the directed boundary walk of face f is

$$e_1^{\epsilon_1} e_2^{\epsilon_2} \cdots e_n^{\epsilon_n}$$

then the rotation at vertex (f, b) is

$$(e_1, b_1)^{\epsilon_1} (e_2, b_2)^{\epsilon_2} \cdots (e_n, b_n)^{\epsilon_n}$$

where $b_i = b$ if $\epsilon_i = +$, and $b_i = b\beta(e_i^-)$ if $\epsilon_i = -$. This rotation is more easily denoted

$$(e_1^{\epsilon_1}, b)(e_2^{\epsilon_2}, b) \cdots (e_n^{\epsilon_n}, b).$$

Observe that the rotation at vertex (f, ab) is obtained from the rotation at vertex (f, b) by multiplying all $\mathscr{R}$ coordinates on the left by a.

Example 4.4.1 Revisited. *For $j = 1, \ldots, 9$, let e_j be the edge whose plus direction carries the current j. Gustin's method of obtaining a generating row is clearly no more than an application of the Face Tracing Algorithm. Thus the base imbedding $G \to S$ has one face whose directed boundary walk is*

$$e_9 e_7 e_8 e_3 e_6^- e_4^- \ldots$$

Denote this face by v. For $j = 1, \ldots, 9$ and $i = 1, \ldots, 19$, the derived edge $(e_j, i)^+$ runs from vertex (v, i) to vertex $(v, i + j)$. Thus, the derived graph is the complete graph K_{19}. The rotation at vertex $(v, 0)$ is

$$(v,0).\quad (e_9,0)(e_7,0)(e_8,0)(e_3,0)(e_6,13)^-(e_4,15)^- \ldots$$

Since the derived graph is simplicial, this rotation can also be given in vertex form. If we let $v_i = (v, i)$, the result is

$$v_0.\quad v_9 v_7 v_8 v_3 v_{13} v_{15} \ldots$$

which is the generating row given by Gustin's construction. Moreover, the full rotation system is also the same as Gustin's scheme, since the rotation at vertex v_i is obtained from that at vertex v_0 by adding i modulo 19 to all $\mathscr{R}$ coordinates.

Example 4.4.2 (Jungerman, 1975). *Consider the current graph $\langle G \to S, \beta \rangle$ given by Figure 4.19, where the current group is $\mathscr{Z}_{16}$. An application of the Face Tracing Algorithm shows that the base imbedding has two faces, which we denote u and v, and that vertices u_0 and v_0 of the derived imbedding have the following rotations:*

$$u_0.\quad v_3 u_2 v_{15} u_6 v_7 v_5 v_{11} v_{13} u_{14} v_1 u_{10} v_9$$
$$v_0.\quad u_3 v_{14} u_9 u_{15} u_{13} v_6 u_{11} v_2 u_5 v_{10} u_7 u_1$$

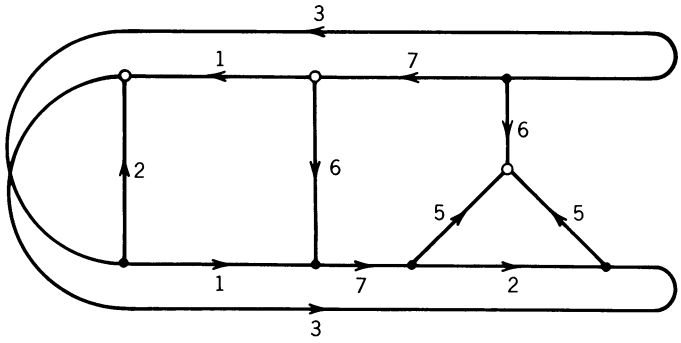

Figure 4.19. A current graph with currents in $\mathscr{Z}_{16}$.

An inspection of these two rows reveals that the vertex u_i is adjacent to the vertex v_j if and only if $j - i$ is odd, and that u_i is adjacent to u_j (similarly v_i and v_j) if and only if $j - i \equiv 2 \bmod 4$. It follows that $\{u_i: i \text{ even}\} \cup \{v_j: j \text{ odd}\}$ is the vertex set for one component of the derived graph. In this component, every pair of vertices is adjacent except u_i and u_j, where $j - i \equiv 0 \bmod 4$ and v_i and v_j, where $j - i \equiv 0 \bmod 4$. Thus, this component is isomorphic to the complete multipartite graph $K_{4,4,4,4}$. The other 16 vertices of the derived graph lie in a second copy of $K_{4,4,4,4}$.

4.4.4. Faces of the Derived Graph

Just as the vertices of a derived graph correspond to the faces of its current graph, faces of a derived graph correspond to vertices of its current graph. The proof of the following theorem is postponed to the next section, where it is shown to be a simple consequence of the duality between current and voltage graphs. Originally, the theorem was proved by an application of the Face Tracing Algorithm to the derived imbedding.

Theorem 4.4.1 (Gross and Alpert, 1974). *Let $e_1^{\epsilon_1} \ldots e_n^{\epsilon_n}$ be the rotation at vertex v of the current graph $\langle G \to S, \beta \rangle$, and let c_i be the current carried by the direction of the edge e_i that has v as its initial vertex. Let $c = c_1 \ldots c_n$, and let r be the order of c in the current group $\mathscr{B}$. Then the derived imbedding has $\#\mathscr{B}/r$ faces corresponding to vertex v, each of size rn, and each of the form*

$$(e_1^{\epsilon_1}, b), (e_2^{\epsilon_2}, bc_1), (e_3^{\epsilon_3}, bc_1c_2) \ldots (e_n^{\epsilon_n}, bc_1c_2 \ldots c_{n-1})$$
$$(e_1^{\epsilon_1}, bc), (e_2^{\epsilon_2}, bcc_1), (e_3^{\epsilon_3}, bcc_1c_2) \ldots$$
$$\vdots$$
$$(e_1^{\epsilon_1}, bc^r) = (e_1^{\epsilon_1}, b) \quad \square$$

The product $c_1 \ldots c_n$ in Theorem 4.4.1 is called the excess current at vertex v. The Kirchhoff current law (KCL) holds at vertex v if the excess current is the identity.

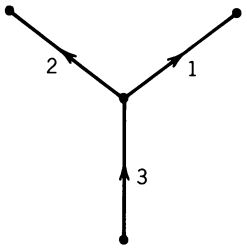

Figure 4.20. A current graph with currents in $\mathscr{Z}_6$.

Corollary. *Let $\langle G \to S, \beta \rangle$ be a current graph such that KCL holds at every vertex and every vertex has valence three. Then the derived imbedding is triangular.* □

Since KCL holds at every vertex in both Example 4.4.1 and Example 4.4.2, both derived imbeddings are triangular. Thus the first gives a minimal-genus imbedding of K_{19}, whereas the second gives a minimal-genus imbedding of $K_{4,4,4,4}$.

Example 4.4.3. *The current graph given in Figure* 4.20 *with currents in $\mathscr{Z}_6$ has one face, denoted v. By face tracing, we see that the rotation at vertex v_0 of the derived imbedding is*

$$v_0. \quad v_2\, v_4\, v_1\, v_5\, v_3\, v_3$$

The order of the excess current at the bottom vertex of the current graph is 2. *If we excise the resulting three digons of the derived imbedding and reclose the surface by identifying opposite sides, we thereby identify three pairs of multiple edges from v_i to v_{i+3}, for $i = 1, 2, 3$. The final product is an imbedding of the complete graph K_6. The* 3*-valent vertex of the current graph satisfies KCL and it generates six triangles, and the two remaining* 1*-valent vertices together yield one hexagon and two triangles. Thus, the Euler characteristic of the derived surface is* $6 - 15 + 9 = 0$. *The scheme whose generating row is the given rotation for v_0 with the extra v_3 deleted is precisely the table Heffter gives for his minimal-genus imbedding of K_6.*

Example 4.4.4. *Consider the current graph given in Figure* 4.21 *with currents in the cyclic group $\mathscr{Z}_{100}$. There are two faces, which we denote u and v. In the derived graph, there is an edge between u_i and v_{i+1} for all i, and there are no other edges. Therefore the derived graph has two components; the vertex set of one component is*

$$\{u_i\colon i \text{ even}\} \cup \{v_j\colon j \text{ odd}\}$$

Each vertex of the current graph has excess current ± 2 *and valence* 2, *and thereby generates a pair of* 100*-gons; each of these* 100*-gons passes through every vertex in its component. Add a vertex inside each of the six* 100*-gons of one*

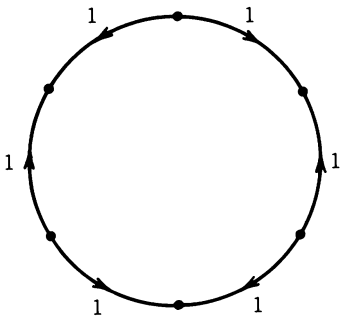

Figure 4.21. A current graph with currents in $\mathscr{Z}_{100}$.

component, and add edges joining that vertex to the 100 *original vertices. Then delete all the original edges. The resulting graph is the complete bipartite graph* $K_{6,100}$, *and every face of the resulting imbedding is a quadrilateral. Hence the imbedding has minimal genus.*

Clearly, Example 4.4.4 generalizes to arbitrary even integers m and n, yielding quadrilateral and hence minimal-genus imbeddings of $K_{m,n}$ for these cases. Exercise 11 shows how quadrilateral imbeddings of $K_{m,n}$ can be obtained when m is odd and $n \equiv 2 \bmod 4$.

4.4.5. Nonorientable Current Graphs

It is possible to consider current graphs in nonorientable surfaces as well. The difficulty is that vertex rotations are reversed by type-1 edges during the Face Tracing Algorithm, so care must be taken in using vertex rotations to define the derived graph. For instance, suppose that e is a type-1 edge lying between faces f and g, as illustrated in Figure 4.22. Unlike the orientable case, the rotation at either endpoint of edge e sends face f to face g. If e^+ carries current c and e^- were to carry current c^{-1}, then in the derived graph, there would be edges corresponding to e running from vertex (f, b) to both of the vertices (g, bc) and (g, bc^{-1}). Therefore, both directions of a type-1 edge must be assigned the same current. Also, in tracing faces of the derived graph, the edge e is traversed in the same direction twice; it follows that in computing the excess currents at the endpoints of edge e, the current c must be used twice. Thus type-1 edges in nonorientable current graphs ("cascades" in Youngs's terminology) appear in print with arrows in both directions.

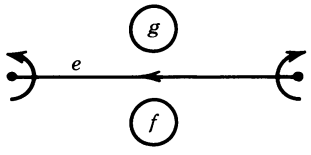

Figure 4.22. A type-1 edge.

problem. However, only orientable case 7 admits such a direct construction, and even in that case, it requires considerable ingenuity to assign the voltages correctly to the imbedded base graph. Each of the other three regular orientable cases requires a few additional tactics beyond the basic strategy.

5.2.1. A Base Imbedding for Orientable Case 7

Suppose that $n = 12s + 7$. Then the complete graph K_n has $12s + 7$ vertices and $(12s + 7)(6s + 3)$ edges. Our objective is to construct an imbedding with $(12s + 7)(4s + 2)$ faces, every one a triangle. The greatest common divisor of these three numbers is $12s + 7$, so the obvious approach is to consider a base graph imbedding such that

$$\#V = 1 \quad \#E = 6s + 3 \quad \text{and} \quad \#F = 4s + 2$$

that is, an imbedding of the bouquet B_{6s+3} in the surface S_{s+1}.

There is little trouble in constructing candidates for a base imbedding, if one generalizes a construction for surfaces already considered in Figure 4.31. In that figure, opposite sides of an octagon are pasted to each other to produce the surface S_2. In general, the opposite sides of a $4g$-sided polygon can be pasted together to yield the surface S_g. To prove that this works, one considers the corners of the polygon to be vertices of a graph and the sides of the polygon to be edges. The result of the pasting leaves $2g$ edges and one face, obviously. It is not difficult to verify that it also leaves only one vertex. (See Exercises 1–3.) Thus the result is the bouquet B_{2g} imbedded in the orientable surface of Euler characteristic $1 - 2g + 1$, that is, the surface S_g.

To obtain an imbedding of the bouquet B_{6s+3} in the surface S_{s+1}, one begins with a $(4s + 4)$-sided polygon. When each side is pasted to the opposite side, the result is an imbedding $B_{2s+2} \to S_{s+1}$. If one now draws a line from one corner of the $(4s + 4)$-sided face to each of the other $4s + 1$ corners to which it is not adjacent, one obtains an imbedding $B_{6s+3} \to S_{s+1}$. The scallop-shell appearance of this imbedding is illustrated in Figure 5.4.

Ordinarily one tries to choose the voltage group to be cyclic, since cyclic groups are the least complicated. In this case, since the covering space to be constructed is $(12s + 7)$-sheeted, the obvious candidate for a voltage group is $\mathscr{Z}_{12s+7}$. Moreover, since numbers of the form $12s + 7$ can be prime, the only hope to lift some of the scallop-shell base imbeddings to triangular imbeddings of complete graphs is with cyclic voltage groups.

Any one-to-one assignment of the voltages $1, \ldots, 6s + 3$ modulo $12s + 7$ to the edges of the bouquet B_{6s+3} yields K_{12s+7} as the derived graph. However, they must be assigned so that the Kirchhoff voltage law holds globally, else the derived imbedding would not be a triangulation. There is no known general reason to suppose that a particular problem of this kind can be solved at all.

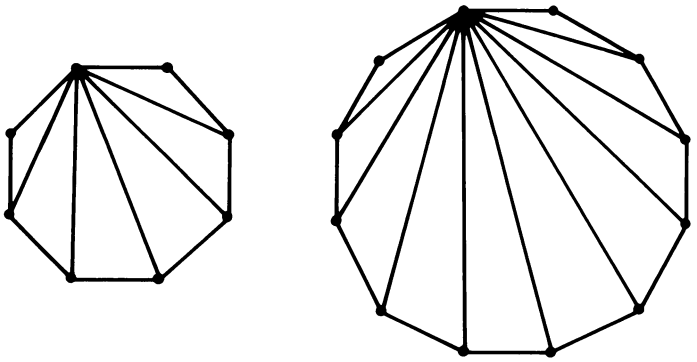

Figure 5.4. Imbeddings $B_9 \to S_2$ and $B_{15} \to S_3$. These are base graphs for imbeddings $K_{19} \to S_{20}$ and $K_{31} \to S_{64}$.

Alternatively, one may observe that the global Kirchhoff voltage law corresponds to a system of $4s + 2$ linear equations in $6s + 3$ unknown edge-voltages, which would seem to have many solutions. However, the requirement that each of the voltages $1, \ldots, 6s + 3$ be used exactly once corresponds to an inequality

$$\prod_{i,j}(x_i - x_j) \neq 0$$

of degree $\binom{6s+3}{2}$. Accordingly, one does not expect to find a solution by the routine application of general methods.

5.2.2. Using a Coil to Assign Voltages

To obtain a satisfactory voltage assignment for the scallop shell base imbedding, the voltages $1, \ldots, 6s + 3$ modulo $12s + 7$ are first partitioned into three intervals. Voltages $1, \ldots, 2s$ in the lower range are distributed along the rim of the shell in consecutive clockwise order, with plus edge directions assigned so they alternate. The voltage $2s + 1$ is assigned to the middle interior edge. Voltages $2s + 2, \ldots, 4s + 2$ in the middle range are assigned to the right half of the shell, and voltages $4s + 3, \ldots, 6s + 3$ are assigned to the left half. Figure 5.5 shows the way that they are assigned.

The relationship between the voltages $1, \ldots, 2s$ in the lower range and the voltages $2s + 2, \ldots, 4s + 2$ in the middle range is called a "coil". Note first that the voltage $3s + 2$ in the precise middle of the middle range is assigned to the top edge of the scallop shell. The first outer voltage to follow $3s + 2$ is the voltage 1, and the plus direction of its edge is opposite to that of the top edge. Thus, the top triangle will satisfy *KVL* if and only if $3s + 1$ is assigned to its

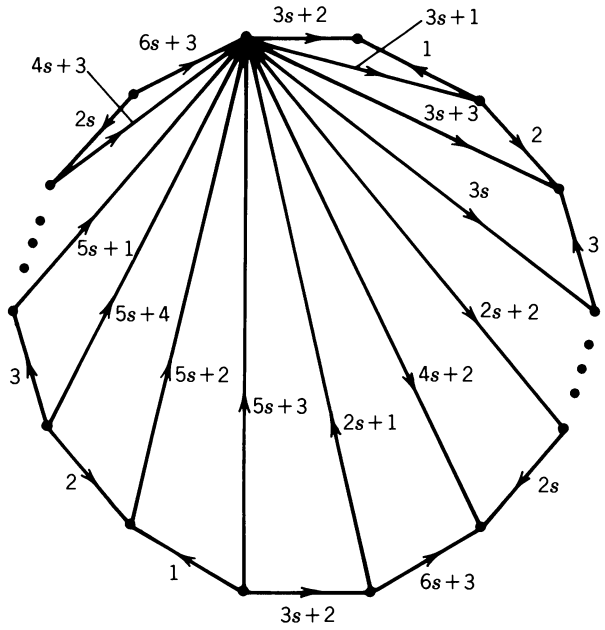

Figure 5.5. This assignment of voltages in $\mathscr{Z}_{12s+7}$ to the imbedded bouquet $B_{6s+3} \to S_{s+1}$ satisfies *KVL* and yields as a derived graph a triangular imbedding $K_{12s+7} \to S_{I(12s+7)}$.

other edge. Since the voltage 2 is assigned to the outer edge of the second triangle from the top, in the same direction as the voltage $3s + 1$, that triangle will satisfy *KVL* if its other edge is assigned the voltage $3s + 3$. In this manner the voltages $1, \ldots, 2s$ are used to coil from the middle voltage $3s + 2$ in the middle range outward to the limiting voltages $2s + 2$ and $4s + 2$. Figure 5.6 shows a combinatorial abstraction of the coil.

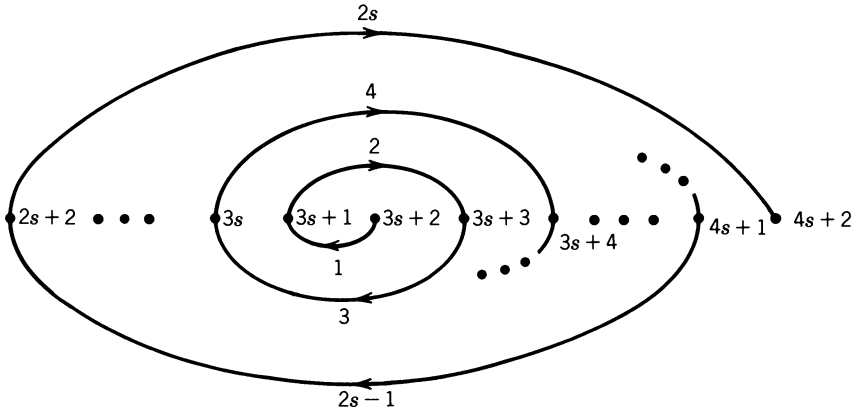

Figure 5.6. The voltages $1, \ldots, 2s$ are used to coil outward from $3s + 2$ toward $2s + 1$ and $4s + 2$.

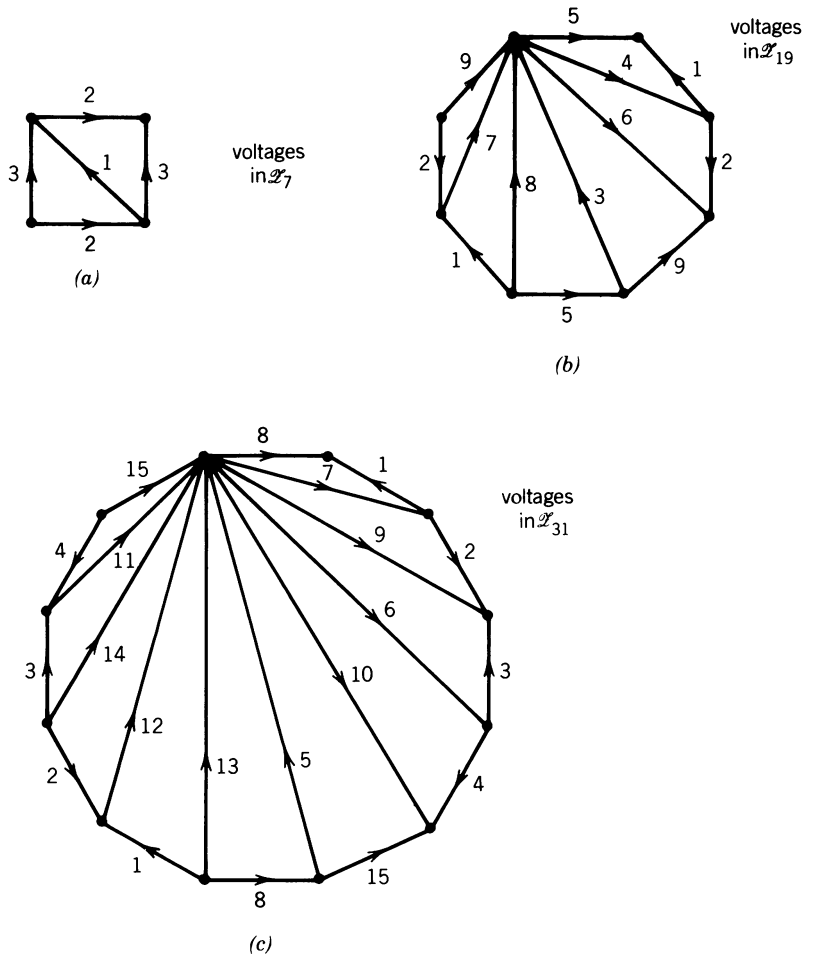

Figure 5.7. Imbedded voltage graphs that yield triangular imbeddings of (a) K_7, (b) K_{19}, and (c) K_{31}.

Because of the way the scallop shell is to be pasted together to form a closed surface, the lower voltages $1, \ldots, 2s$ also appear on the left rim. There they coil among the upper voltages $4s + 3, \ldots, 6s + 3$, starting from $5s + 3$ on the vertical interior edge and working outward. The result is that *KVL* also holds on the triangles on the left side of the shell.

The voltage $2s + 1$ on the middle interior edge welds the two coils together, so that *KVL* is also satisfied on the two triangular faces in which it lies. Thus, *KVL* holds globally, and the Heawood problem is solved for orientable case 7. Figure 5.7 shows the voltage assignments for imbeddings $B_3 \to S_1$, $B_9 \to S_2$, and $B_{15} \to S_3$ that have derived triangular imbeddings $K_7 \to S_1$, $K_{19} \to S_{20}$, and $K_{31} \to S_{63}$, respectively.

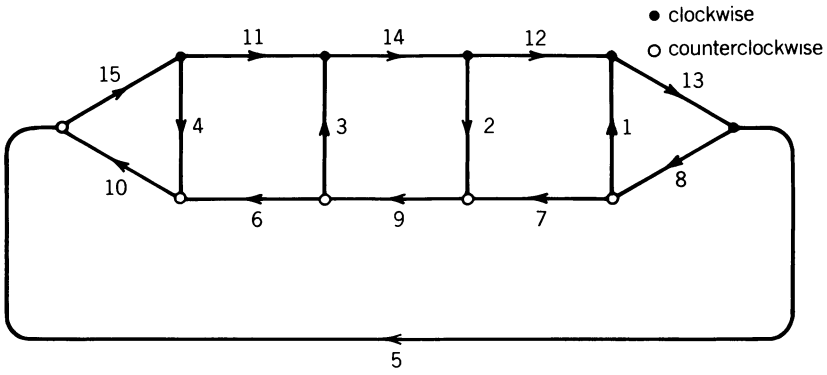

Figure 5.8. A Gustin current graph for K_{31}.

5.2.3. A Current-Graph Perspective on Case 7

If one now draws the dual of the imbedded voltage graph in Figure 5.7*b*, one obtains precisely the topological current graph already illustrated in Figure 4.31. The underlying graph is planar and 3-regular, so that it is also possible to draw an equivalent Gustin current graph in the plane, with no edge-crossings. Such a Gustin current graph appears in Figure 4.18. Figure 5.8 shows the Gustin current graph that is equivalent to the imbedded voltage graph in Figure 5.7*c*.

The coiling relationship among the currents is highly visible in this ladder-like Gustin current graph. It is also easy to see that *KCL* is satisfied at every vertex. This ease of visibility makes Gustin current graphs very useful in computations. On the other hand, while the base graph imbedding for the voltage graph solution is designed to have one vertex, it requires a certain amount of work to check the corresponding face in the Gustin current graph.

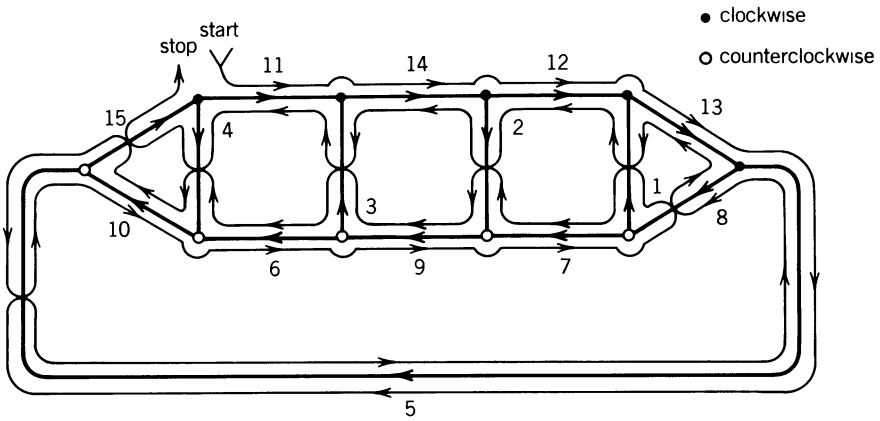

Figure 5.9. Pictorial representation of the Face Tracing Algorithm.

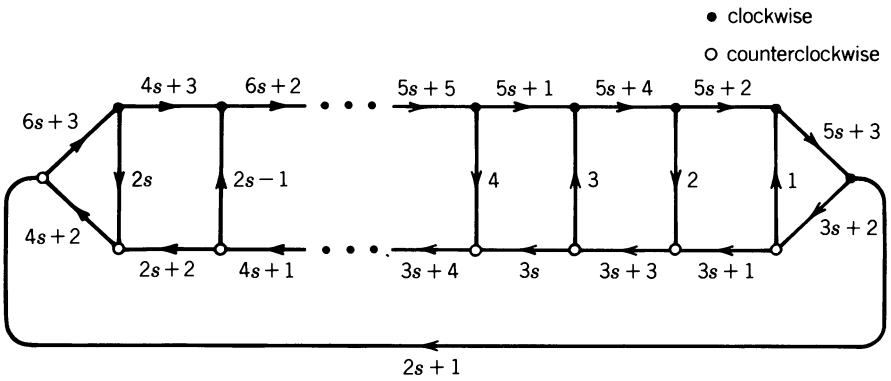

Figure 5.10. A general current graph for orientable case 7 of the Heawood problem.

Fortunately, there is a pictorial way to apply the Face Tracing Algorithm, illustrated in Figure 5.9.

One may start at any edge. In this example, we have started with the horizontal edge at the upper left, which carries the current 11. Since the terminal vertex of that edge is solid, the next edge we traverse is the one carrying the current 14. When this single edge orbit closes on itself, every edge has been traversed in both directions. Thus, the corresponding imbedding has only one face. The thin line that runs along the edges in Figure 5.9 traces out the boundary circuit of that face.

The general voltage graph for orientable case 7, shown in Figure 5.5, also has a dual that may be represented as a ladderlike Gustin current graph. This is shown in Figure 5.10. Ringel (1961) solved this case with purely combinatorial methods. The generating row he devised anticipates the technique of coiling.

5.2.4. Orientable Case 4: Doubling 1-Factors

If $n = 12s + 4$, then the complete graph K_n has $12s + 4$ vertices and $(6s + 2)(8s + 2)$ triangular faces. Since the greatest common divisor of these three numbers is $6s + 2$, the obvious properties one might want in an imbedded voltage graph are 2 vertices, $12s + 3$ edges, and $8s + 2$ triangular faces. Unfortunately, the complete graph K_{12s+4} cannot have such a quotient.

Theorem 5.2.1 (Gross and Tucker, 1974). *Let p: $K_n \to G$ be a covering projection. Then the cardinality of the fibers is an odd number.*

Proof. Let v be a vertex of the base graph G. Suppose that there are $2n$ vertices in the fiber over v. Then the subgraph of G spanned by these $2n$ vertices is isomorphic to K_{2n} and contains $n(2n - 1)$ edges. These $n(2n - 1)$ edges must be the union of the fibers of v-based loops. However, every edge fiber contains $2n$ edges, and $2n$ does not divide $n(2n - 1)$, a contradiction. □